Published in final edited form as:
Organometallics. 2008 January ; 27(1): 119–125.

Desymmetrized Diiron Azadithiolato Carbonyls: A Step Toward Modeling the Iron-Only Hydrogenases

Jane L. Stanley,
Department of Chemistry, University of Illinois at Urbanas—Champaign, Urbana, Illinois 61801

Zachariah M. Heiden,
Department of Chemistry, University of Illinois at Urbanas—Champaign, Urbana, Illinois 61801

Thomas B. Rauchfuss*,
Department of Chemistry, University of Illinois at Urbanas—Champaign, Urbana, Illinois 61801

Scott R. Wilson,
Department of Chemistry, University of Illinois at Urbanas—Champaign, Urbana, Illinois 61801

Luca De Gioia, and
Department of Biotechnology and Biosciences, University of Milano-Bicocca, Piazza della Scienza 1, 20126-Milan, Italy

Guiseppe Zampella
Department of Biotechnology and Biosciences, University of Milano-Bicocca, Piazza della Scienza 1, 20126-Milan, Italy

Abstract

Condensation of $Fe_2(SH)_2(CO)_6$, acetaldehyde, and $(NH_4)_2CO_3$ affords the methyl-substituted azadithiolate $Fe_2[(SCHMe)_2NH](CO)_6$ (**1**). The complex exists mainly (~95%) as the meso diastereomer, but the *d*,*l* diastereoisomers could be detected. DFT calculations predict that the meso isomer would be 2.5 kcal/mol more stable than the *d*,*l* isomer due to conventional nonbonding interactions between the methyl groups and the ring hydrogen atoms. Crystallographic analysis of *meso*-**1** confirms that the two methyl groups are equatorial, constraining the diferraazadithiolate bicycle to a conformation that desymmetrizes the diiron center. The lowered symmetry is confirmed by the observation of two ^{13}C NMR signals in the Fe*C*O region under conditions of fast turnstile rotation at the $Fe(CO)_3$ groups. The pK_a value of the amine in **1** is 7.89 (all pK_a's determined in MeCN solution), which is similar to a redetermined value for $Fe_2[(SCH_2)_2NH](CO)_6$ (**2**, pK_a = 7.98) and only slightly less basic than the tertiary amine $Fe_2[(SCH_2)_2NMe](CO)_6$ (pK_a = 8.14). Substitution of **1** with PMe_3 proceeded via the intermediacy of two isomers of $Fe_2[(SCHMe)_2NH](CO)_5(PMe_3)$, affording $Fe_2[(SCHMe)_2NH](CO)_4(PMe_3)_2$ (**3**). ^{31}P NMR spectra confirm that the two PMe_3 ligands in **3** are nonequivalent, consistent with the desymmetrizing effect of the dithiolate. The pK_a value of the amine in **3** was found to be 11.3. Using triphenylphosphine, we prepared $Fe_2[(SCHMe)_2NH](CO)_5(PPh_3)$ as a single regioisomer.

*To whom correspondence should be addressed. E-mail: rauchfuz@uiuc.edu.

Supporting Information Available: Text, tables, and figures giving NMR spectra of PMe_3 and PPh_3 adducts of **1**, low-temperature NMR spectra of **1** and *d*,*l*-**1**, kinetic data for the tautomerization of $[Fe_2[(SCHMe)_2NH_2](CO)_4(PMe_3)_2]^+$ and $[Fe_2[(SCH_2)_2NH_2](CO)_4(PMe_3)_2]^+$, details of p$K_a$ determinations, and results from DFT calculations and CIF files giving crystallographic data for $Fe_2[(SCH_2)_2NH]CO)_6$, $Fe_2[(SCHMe)_2NH](CO)_6$, and $Fe_2[(SCHMe)_2NH](CO)_5(PPh_3)$. This material is available free of charge via the Internet at http://pubs.acs.org.

Introduction

The iron-only hydrogenases have attracted intense attention from the organometallic community because of the unusual structure of their active sites and the prevailing interest in the coordination of dihydrogen.[1] The enzyme converts protons to H_2 with extraordinary efficiency,[2] which has motivated interest in developing new catalysts.[3] The active site is only lightly attached to the protein; thus, models do not require, a priori, the incorporation of peptidomimetic ligands. One overarching challenge in the modeling efforts arises from the fact that the two Fe centers are usually equivalent in most models but inequivalent in nature. Biophysical measurements indicate that substrate binding occurs only at the "distal" Fe center, the one more distant from the [4Fe-4S] cluster.[4] Furthermore, protein crystallography indicates that the surrounding protein funnels substrates and products to and from one particular axial site on the distal Fe (Scheme 1).

The azadithiolato and the isosteric 1,3-propanedithiolato ligands in model compounds rapidly undergo a degenerate conformational equilibrium that equivalences the two Fe centers (Scheme 1).[5] Synthetic routes to diiron azadithiolato compounds, however, present opportunities to "desymmetrize" the binuclear center by making one Fe stereochemically distinct from the other. In diiron azadithiolates, one could in principle replace the methylene spacer with an ethylidene, thereby generating conformationally biased dithiolates. Such derivatives would distinguish the two iron centers with respect to their adjacency to the amine. Complementary to this idea, considerable recent work has focused on desymmetrizing diiron dithiolates by installing ligands unsymmetrically.[6,7]

The presence of bulky substituents adjacent to the thiolates could enhance the stability of these complexes. Both theoretical[8] and experimental studies[9] indicate that the thiolato sulfur atoms in diiron dithiolato carbonyls are susceptible to attack by electrophiles.

Results

Synthesis of $Fe_2[(SCHMe)_2NH](CO)_6$

We found that the condensation of $Fe_2(SH)_2(CO)_6$, acetaldehyde, and $(NH_4)_2CO_3$ affords the azadithiolate $Fe_2[(SCHMe)_2NH](CO)_6$ (**1**). The ammonia source and the aldehyde were allowed to prereact, followed by the addition to the diiron dithiol. Proceeding in ca. ~45% yield, the reaction is more efficient than the synthesis of the parent $Fe_2[(SCH_2)_2NH](CO)_6$ (**2**).[10] Compound **1** was also prepared by treating $Fe_2(SH)_2(CO)_6$ with the cyclic trimer $(MeCHNH)_3$;[11] this method is slightly faster but offered no other advantages (eq 1).

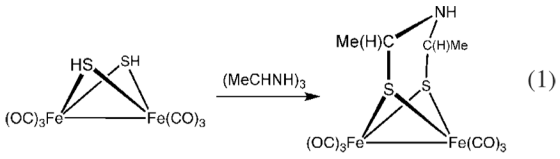

(1)

IR spectra in the ν_{CO} region for **1** and **2** are very similar: the bands for the dimethylated complex are lower in energy by ~2 cm^{-1}, and they have similar basicities (see below). The room-temperature ^{13}C NMR spectrum for **1** showed two *C*O signals, whereas only one band was observed for **2** (Supporting Information, Figure S2).

In principle, a range of aldehydes could be used in place of acetaldehyde. Preliminary evidence confirms that such reactions do occur, but the products are often unstable. For example, the condensation using PhCHO in place of MeCHO gave multiple products that decomposed upon workup. Using *t*-$BuNH_2$ in place of ammonia appeared to afford $Fe_2[(SCHMe)_2NBu\text{-}t]$

$(CO)_6$, as indicated by IR and ESI-MS analysis (Supporting Information, Figure S8). This species also proved less stable than **1**.

The structure of the major diastereoisomer of **1** was confirmed crystallographically. This isomer is meso (*R*,*S*) with C_s symmetry (Scheme 2).

The methyl groups are equatorial with respect to the bicyclic $Fe_2S_2C_2N$ ring (Figure 1). The N—*H*, which was located crystallographically, is axial with respect to the bicyclic $Fe_2S_2C_2N$ ring and approximately parallel to the Fe—Fe bond, as is commonly observed for related azadithiolates.[12] For the sake of comparison, we also determined the structure of the parent azadithiolate **2** (Supporting Information, Figure S1). Differences between the two structures are minor; only a slight expansion of the C—N—C angle by 1.5° (see Table 1) is observed in **1** and a decrease in the S—Fe—S angle of ~29°.

d,l-$Fe_2[(SCHMe)_2NH](CO)_6$

In addition to *meso*-**1**, the condensation reaction could also produce the chiral *d,l* isomer (Scheme 2). Fresh $CDCl_3$ solutions of **1** indicate the presence of only the meso isomer, although upon warming to 45 °C, up to 10% of the second isomer appears concomitant with some decomposition. In acetonitrile, the *d,l* isomer was present at the level of ca. 8% (Supporting Information, Figure S3). This minor isomer was characterized by its ^1H NMR spectrum as a minor component in samples of **1**. At −45 °C, two methyl doublets are apparent, consistent with one being axial and one equatorial. At 75 °C, the doublets were found to coalesce into a single doublet (Supporting Information).

DFT Investigation of $Fe_2[(SCHMe)_2NH](CO)_6$

The relative energies of the achiral isomers exhibiting diaxial methyl groups and diequatorial methyl groups, as well as the chiral isomer of $Fe_2[(SCHMe)_2NH](CO)_6$, were evaluated using DFT calculations. The observed diequatorial structure is more stable than the *d,l* isomer by 2.5 kcal/mol (298 K, $K_{eq} = 64$). The diaxial conformer of the meso disastereomer is particularly destabilized, being 6.6 kcal/mol less stable than the meso-diequatorial conformer (eq 2, Figure 2). The stability ranking of the different isomers can be rationalized in light of standard steric considerations valid for substituted six-membered saturated rings, as confirmed by the relative stabilities computed for the isomers of $CH_2(SCHMe)_2NH$ (see Supporting Information), which are in agreement with thermochemical studies on 2,6-dimethylpiperidine.[13]

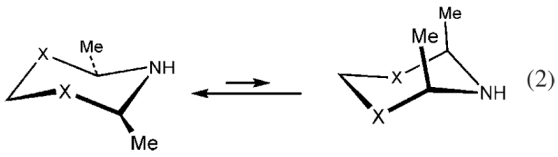

(2)

The NH group in $Fe_2[(SCHMe)_2NH](CO)_6$ isomers is predicted to adopt an axial orientation, as observed in related diiron azadithiolato complexes.[14]

The Substituted Derivatives: $Fe_2[(SCHMe)_2NH](CO)_{6-x}(PR_3)_x$

The substitution reactions of **1** allowed us to assess the influence of desymmetrization on the reactivity of the underlying $Fe(CO)_3$ centers. Solutions of **1** were found to react with excess PMe_3 to give mono- and disubstituted derivatives. The ^{31}P NMR spectrum of the bisphosphine complex is consistent with nonequivalent $Fe(CO)_2(PMe_3)$ centers, as a consequence of the desymmetrization (Supporting Information, Figure S5).

The regioselectivity of the reaction of **1** and PMe_3 was evaluated by in situ ^{31}P NMR measurements. We observed a ~3:1 ratio of two monophosphine complexes, which we assign to the isomers of $Fe_2[(SCHMe)_2NH](CO)_5(PMe_3)$ that have the phosphine near or away from the amine, respectively. At longer reaction times, these two singlets disappeared concomitant with the appearance of the signals corresponding to $Fe_2[(SCHMe)_2NH](CO)_4(PMe_3)_2$ (Supporting Information, Figure S6). We also observed the growth of a singlet that did not disappear. This species may have been *d,l*- $Fe_2[(SCHMe)_2NH](CO)_5(PMe_3)$, but this species did not persist in the recrystallized product. The selectivity of the substitution reactions increased when PPh_3 was employed as the nucleophile. In this case, we obtained only a single isomer (^{31}P NMR: δ 66.2) of $Fe_2[(SCHMe)_2NH](CO)_5(PPh_3)$ where the phosphine is located on the iron center that is not shielded by the amine (eq 3).

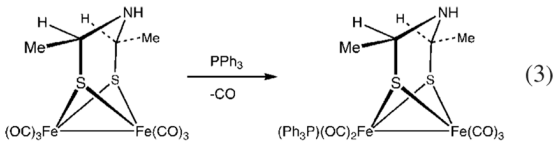

(3)

The structure of *meso*-$Fe_2[(SCHMe)_2NH](CO)_5(PPh_3)$ was confirmed crystallographically (Figure 3, Table 1). Relative to the numerous precedents of azadithiolates, the monophosphine complex has an unremarkable structure. The phosphine is located on the more open iron center, trans to the Fe—Fe bond. In the absence of severe steric interactions, it is typical for donor ligands to be positioned in the apical positions, trans to the Fe—Fe bond[15] but isomers have been observed with phosphine ligands located at basal sites.[16,17]

Basicity of the Amine in $Fe_2[(SCHR)_2NR'](CO)_{4-x}(PMe_3)_x$ (x = 0, 2; R = Me, H)

The protonation of the amine in **1** can be monitored by shifts in the ν_{CO} bands in the IR spectrum (Figure 4). *N*-protonation induced shifts in ν_{CO} of ca. 15 cm^{-1} to higher energy. Similar shifts have been shown to be associated with *N*-protonation of related azadithiolatodiiron complexes.[11,13,15,16] One *N*-protonated azadithiolato complex, $[Fe_2[(SCH_2)_2N(C_6H_4\text{-}2\text{-}Br)H](CO)_6]ClO_4$, has been characterized crystallographically.[18] It is interesting that the protonation of **1** affects all of the CO bands; one might expect a greater effect on CO ligands nearer to the ammonium center. Indeed, DFT calculations of CO vibrational frequencies (Supporting Information, Table S1) show that the *N*-protonation induced shifts for the six CO vibrational bands is quite uniform, reflecting the fact that the CO vibrational normal modes are generally highly coupled.

From IR spectra in the ν_{CO} region, it was apparent that the acidities of the ammonium compound $\mathbf{1}H^+$ and anhydrous *p*-toluenesulfonic acid (HOTs, 8.7 in MeCN)[19] are comparable. Compounds **2** and $Fe_2[(SCH_2)_2NMe](CO)_6$ are similar in basicity as well, consistent with the near-equivalent basicity normally seen for related secondary and tertiary alkylamines.[19] Using titrations that were monitored by IR spectroscopy, we determined the pK_a's (Table 2) after correcting for homoconjugation between HOTs and OTs^- and, less severely, $PhNH_3^+$ and $PhNH_2$ (where the homoconjugation constant, k^f = 2.95 and 0.60 in MeCN, respectively).[19]

The presence of the phosphine ligands was found to influence the basicity of the amine. This point was established by examining the protonation of $Fe_2[(SCHMe)_2NH](CO)_4(PMe_3)_2$ in MeCN solution. In contrast to the case for the parent hexacarbonyl, this species was fully protonated with 1 equiv of HOTs (Figure 5). A solution of $[Fe_2[(SCHMe)_2NH_2](CO)_4(PMe_3)_2]^+$ was half-deprotonated by aniline, indicating a pK_a value of at least ~10. Using a titration with $PhNH_3OTf$ (pK_a = 10.56 in MeCN),[19] we refined this value to 11.29 (Table

2). This value is similar to the result of Ott et al., whose $[Fe_2[(SCH_2)_2NH(CH_2Ph)](CO)_4(PMe_3)_2]^+$ complex was found to have a pK_a value of 12.[20]

In MeCN solution $[Fe_2[(SCHMe)_2NH_2](CO)_4(PMe_3)_2]^+$ was found to slowly tautomerize to the isomer containing a bridging hydride, $[Fe_2[(SCHMe)_2NH](\mu\text{-}H)(CO)_4(PMe_3)_2]^+$. This isomerization was signaled by a shift of ~30–35 cm^{-1} in ν_{CO} to higher energies (Figure 5, eq 4). The IR spectra for $[Fe_2[(SCHR)_2NH](\mu\text{-}H)(CO)_4(PMe_3)_2]^+$ are identical for R = H and Me (2030 and 1988 cm^{-1}) and very similar to those reported by both Ott et al. for $[Fe_2[(SCH_2)_2NCH_2Ph](\mu\text{-}H)(CO)_4(PMe_3)_2]^+$ (2033 and 1992 cm^{-1})[20] and Wei and Sun for $[Fe_2[(SCH_2)_2NCH_2C_6H_4Br](\mu\text{-}H)(CO)_4(PMe_3)_2]^+$ (2031 and 1991 cm^{-1}).[17] As previously reported,[16] chloride was found to accelerate tautomerization to the hydride.

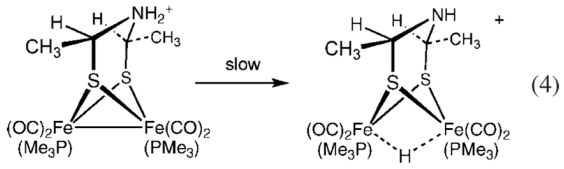

(4)

We investigated the uncatalyzed tautomerization process for the dimethylazadithiolato complex and the simpler azadithiolate. Thus, a solution of the two azadithiolato cations was monitored in the hydride region of the ^1H NMR spectrum. The isomerizations were approximately first order, with that for the $(SCHMe)_2NH$ derivative ($k \approx 6 \times 10^{-6}$ s^{-1}) being 1.5× slower than for the unmethylated derivative (Supporting Information, Figures S10 and S11).

Summary and Conclusions

The condensation of $Fe_2(SH)_2(CO)_6$with formaldehyde—ammonia was extended to develop desymmetrized diiron dithiolates. Not only does this simple method afford the desired product with acceptable stereoselectivity but also the efficiency of the transformation exceeds that of the formaldehyde-based condensation. As judged by crystallographic comparisons as well as pK_a's, the introduction of a pair of methyl groups into the azadithiolate backbone stabilized one particular conformation of the diiron species without significantly distorting the framework or modifying its basicity. The steric impact of desymmetrization is modest for small ligands such as PMe_3, but with the larger PPh_3 we obtained a single isomer of the monosubstituted derivative. This result also has implications for the rates of substitution of the related propanedithiolato and azadithiolato complexes: entering ligands will avoid the iron center most shielded by the dithiolate. The dithiol $HSCHMeCH_2CHMeSH$ is isosteric with $(SCHMe)_2NH$, although it would require separation into the two diastereomers.[21]

In this study we also evaluated the influence of substituents on the basicity of the amine in the azadithiolates. The basicity of the amines in the hexacarbonyl complexes is relatively low, with p$K_a \approx 8$, approximately 11 pK_a units less than for diethylamine (18.8).[19] We had initially estimated that the pK_a value would be much lower.[12] We also verified that coligands on the diiron center increased the basicity of the amine significantly, which was also noted by Ott.[20] The effect of coligands on $(SCHMe)_2NH$ is of interest since, in the [FeFe]-hydrogenases, the iron centers are bound also to two cyanides and a [4Fe-4S] cluster, not six CO's. One can anticipate that the pK_a value of the azadithiolato ligand would be several units above 12 (MeCN scale) for a subferrous version of the active site: i.e., $\{Fe_2[(SCH_2)_2NH](CN)_2(CO)_3(L)\}^{2-}$, where L is a [4Fe-4S] cluster. Using the usual approximation that aqueous pK_a's are 8–9 units lower than for acetonitrile, then the azadithiolate would be expected to have pK_a ~4–6 in water.[22]

Experimental Section

General methodologies, including revised routes to $Fe_2S_2(CO)_6$ and $Fe_2[(SCH_2)_2NH](CO)_6$, were described recently.[7,10] Low-resolution FD-MS was performed by the University of Illinois Mass Spectrometry Laboratory using an 8 kV Micromass 70-VSE instrument. Commercial HOTs · H_2O was dehydrated by maintaining the molten liquid under a dynamic vacuum (ca. 0.1 mmHg) at ~100 °C for 6 h. Hydrated acetaldehyde—ammonia trimer, $(MeCHNH)_3 \cdot 3H_2O$, was used as received from Acros. Unless otherwise stated, chromatography was conducted in air on 10 × 3 cm columns of silica gel (Silicycle, 40–63 μm). Single crystals of $Fe_2[(SCH_2)_2NH](CO)_6$ were grown from concentrated hexane solutions at −20 °C.

$Fe_2[(SCHMe)_2NH](CO)_6$ (1) from Acetaldehyde—-Ammonia Solution

A slurry of 3.60 mL (64.4 mmol) of MeCHO and 3.18 g (33.1 mmol) of $(NH_4)_2CO_3$ in 60 mL of THF was stirred for 1 h. A solution of $Fe_2(SH)_2(CO)_6$ was generated in 50 mL of THF at −78 °C by the usual method from 5.46 g (15.9 mmol) of $Fe_2S_2(CO)_6$, 35.0 mL of a 1 M THF solution of $LiEt_3BH$, and 4.50 mL (58.4 mmol) of CF_3CO_2H. While still cold, the reaction mixture was transferred to the MeCHO—ammonia solution. The reaction was stirred for ca. 14 h, whereupon the color changed from red to deep yellow-brown. The solvent was removed to leave a brown-black oil, which was extracted into hexanes and the extract filtered through Celite to obtain a deep red solution. The red solution was concentrated to 10 mL and purified by silica gel column chromatography with hexanes as eluent to give two red bands. IR spectroscopy indicated that the first band was $Fe_2S_2(CO)_6$. The main product, the second band, was evaporated to yield 2.87 g (44%, assuming perfect conversion of $Fe_2S_2(CO)_6$). The product, which has a pungent odor, sublimes slowly at room temperature under vacuum. Mp: 110.5 °C. IR (hexanes): ν_{CO} 2074, 2033, 2006, 1987, 1976 cm^{-1}. FDMS (*m/z*): 414.9 ($Fe_2[(SCHMe)_2NH](CO)_6^+$). ^1H NMR (CD_3CN) of meso isomer: δ 3.67 (dq, 6.7,13 Hz, SC*H*Me), 1.71 (t, 13 Hz, N*H*), 1.31 (d, 6.7 Hz, CH_3). ^1H NMR (CD_3CN) of *d*,*l* isomer: δ 4.07 (m, SC*H*Me), 2.30 (t, 9 Hz, N*H*), 1.35 (br s, CH_3). ^{13}C NMR (CD_3CN, room temperature): δ 209.6, 208.6, 58.49, 26.45. Anal. Calcd (found) for $C_{10}H_9Fe_2NO_6S_2$: C, 28.94 (28.90); H, 2.19 (1.88); N, 3.38 (3.22). A crystal suitable for X-ray crystallographic analysis was grown from a concentrated MeCN solution at −20 °C. NMR examination of the supernatant from the crystal growth showed that it was not significantly enriched in the *d*,*l* isomer.

$Fe_2[(SCHMe)_2NH](CO)_6$ (1) from Acetaldehyde—Ammonia Trimer

A 60 mL THF solution of $Fe_2(SH)_2(CO)_6$ was generated at −78 °C in the usual way[23] from 1.50 g (4.37 mmol) of $Fe_2S_2(CO)_6$, 9.60 mL of a 1 M THF solution of $LiEt_3BH$, and 1.20 mL (15.6 mmol) of CF_3CO_2H. While still cold, the red solution was transferred to a slurry of 4.79 g (26.1 mmol) of $(MeCHNH)_3 \cdot 3H_2O$ in 35 mL of THF. After it was stirred for 6 h, the reaction mixture was evaporated to give a brown-black oil. The usual workup gave 0.775 g (43%, based on consumed $Fe_2S_2(CO)_6$).

Diastereoisomerization of $Fe_2[(SCHMe)_2NH](CO)_6$

In a typical experiment, a solution of 11.1 mg of $Fe_2[(SCHMe)_2NH](CO)_6$ and 3.3 mg of Ph_3CH (integration standard) were dissolved in 0.74 mL of CD_3CN solution. The *meso*:(*d*/*l*) ratio was 1:0.07 (C*H*Me signals) and 1:0.09 (N*H* signals), corresponding to 7 and 9%, respectively. After the sample was maintained at 50 °C for 1095 min, the *d*/*l* content had decreased to 6.4% and 7.9%, respectively. The conversion was accompanied by significant decomposition of the sample, as indicated by the appearance of a brown precipitate.

$Fe_2[(SCHMe)_2N$-*t*-$Bu](CO)_6$

A 0.33 mL portion (5.90 mmol) of MeCHO and 0.32 mL (0.693 mmol) of *t*-$BuNH_2$ were combined to give a flocculent white slurry, which was diluted with 15 mL of THF and stirred for 1 h. A 25 mL THF solution of $Fe_2(SH)_2(CO)_6$, generated in the usual way from 0.507 g (1.47 mmol) of $Fe_2S_2(CO)_6$, 3.30 mL of a 1 M THF solution of $LiEt_3BH$, and 0.40 mL (5.20 mmol) of CF_3CO_2H, was transferred while still cold into the acetaldehyde—amine solution. After the mixture was stirred for ca. 14 h, the brown oil was extracted with hexanes and the extract filtered through Celite to yield a deep red solution, which was evaporated. The red residue was taken up into 5 mL of 10% CH_2Cl_2 in hexanes and purified by chromatography with the same solvent as eluent to give three red bands, the first being $Fe_2S_2(CO)_6$ and the second an unidentified red oil. The third band was the desired product (further unidentified products could be collected by eluting with CH_2Cl_2). Yield: 0.222 g (32%). IR (hexanes): ν_{CO} 2072, 2033, 2005, 1987, 1977 cm^{-1}. FDMS (*m/z*): 471.0 ($[Fe_2[(SCHMe)_2N$-*t*-Bu](CO)$_6]^+$). After 48 h, almost half of the sample had decomposed, as indicated by TLC on silica gel.

$Fe_2[(SCHMe)_2NH](CO)_4(PMe_3)_2$

A solution of 0.155 g (0.373 mmol) of **1** in 5 mL of MeCN was treated with a solution of 0.0429 g (0.471 mmol) of Me_3NO in 5 mL of MeCN. The reaction solution was then treated with a solution of 0.5 mL (4.92 mmol) of PMe_3 in 10 mL of MeCN. After 10 h at 30 °C, the reaction mixture was evaporated in vacuo. The black solid was purified by anaerobic column chromatography with CH_2Cl_2 as eluent to give two bands. The first band was identified by IR spectroscopy as $Fe(CO)_3(PMe_3)_2$.[24] The second red-purple band, the targeted product, was evaporated to yield a powder. Yield: 0.070 g (37%). ^{1}H NMR (CD_3CN): δ 3.30 (dq, 2H, C*H*Me), 1.22 (d, 6H, CHC*H*$_3$), 1.30 (t, 1H, N*H*), 1.50 and 1.48 (2 d, 18H, PC*H*$_3$). ^{31}P NMR (CD_3CN): δ 29.1(s), 20.1 (s). IR (CH_2Cl_2): ν_{CO} 1980 (w), 1970 (w), 1941 (s), 1898 (br s) cm^{-1}. FD-MS (*m/z*): 511.0 ($[Fe_2[(SCHMe)_2NH](CO)_4(PMe_3)_2]^+$). Anal. Calcd (found) for $C_{14}H_{27}Fe_2NO_4P_2S_2$: C, 32.90 (33.21); H, 5.32 (5.32); N, 2.74 (2.71).

To examine the substitution of **1** by PMe_3, 0.06 mL (0.590 mmol) of PMe_3 was distilled into a frozen solution of 15.5 mg of **1** in 1.01 mL of CD_3CN. The solution was maintained at 50 °C. The 500 MHz ^{31}P NMR spectrum was recorded at 5 min intervals (Supporting Information, Figure S6).

$Fe_2[(SCHMe)_2NH](CO)_5(PPh_3)$

A solution of 0.1002 g (0.241 mmol) of **1** and 0.0634 g (0.242 mmol) of PPh_3 in 10 mL of MeCN was treated dropwise with a solution of 0.0364 g (0.328 mmol) of $Me_3NO \cdot H_2O$ in 5 mL of MeCN. The reaction mixture was stirred at room temperature for 3 h, during which time a red precipitate (the desired product) formed. The supernatant was removed in vacuo. The precipitate was washed with cold MeCN and dried. Further product could be recovered from the dried supernatant, which was taken up into a minimum amount of toluene and purified by column chromatography with toluene as eluent. The first red band eluted contained the desired product. Yield: 0.05 g (32%). ^{1}H NMR (toluene-d_8): δ 7.75 (m, 15H, C_6H_5), 2.38 (m, 2H, C*H*Me), 0.98 (d, 6H, CHC*H*$_3$), 1.13 (t, 1H, N*H*). ^{31}P NMR (toluene-d_8): δ 66.2 (s). IR (toluene): ν_{CO} 2044, 1983, 1956, 1938 cm^{-1}. FD-MS (*m/z*): 649.1 ($[Fe_2[(SCHMe)_2NH](CO)_5(PPh_3)]^+$). Anal. Calcd (found) for $C_{27}H_{24}Fe_2NO_5PS_2$: C, 49.93 (49.69); H, 3.73 (3.70); N, 2.16 (2.07). Crystals were grown from a solution of 60 mg of the sample in 2.0 mL of MeCN at −15 °C.

Tautomerization Competition Reaction between $[Fe_2[(SCHMe)_2NH_2](CO)_4(PMe_3)_2]^+$ and $[Fe_2[(SCH_2)_2NH_2](CO)_4(PMe_3)_2]^+$

A J. Young tube was charged with 5.0 mg (9.78×10^{-3} mmol) of $Fe_2[(SCHMe)_2NH](CO)_4(PMe_3)_2$, 4.7 mg ($9.73 \times 10^{-3}$ mmol) of $Fe_2[(SCH_2)_2NH](CO)_4(PMe_3)_2$, 9.4 mg ($4.19 \times 10^{-2}$ mmol) of Ph_3CH (internal standard), and 3.5 mg (1.84×10^{-2} mmol) of anhydrous HOTs, over which 0.79 mL of CD_3CN was distilled under vacuum. The reaction mixture was kept frozen and not allowed to mix until immediately before insertion into the spectrometer. The sample was allowed to thaw over the course of 2 min and shaken for 15 s before insertion into a Varian U500NB NMR instrument. The reaction was allowed to proceed for 14 h, the mixture being spun at a rate of 20 Hz. The growth of the μ-H peak was monitored for both $Fe_2[(SCHMe)_2NH](CO)_4(PMe_3)_2$ (δ −14.7) and $Fe_2[(SCH_2)_2NH](CO)_4(PMe_3)_2$ (δ −14.4), these signals being integrated against the internal standard (δ 5.61). Data from the first 1 h was omitted in kinetic analysis to ensure thermal equilibrium. A pale red precipitate was noticed after 14 h. The high-field ^1H NMR spectrum (CD_3CN) of $[Fe_2[(SCHMe)_2NH](\mu\text{-}H)(CO)_4(PMe_3)_2]^+$ consists of a pseudotriplet at δ −14.7 (J_{H-P} = 21 Hz), indicating the phosphine ligands are trans dibasal (Supporting Information, Figures S9 and S10).[16] ^{31}P NMR: δ 22.7 (d), 20.7 (d).

Determination of pK_a's

A solution of 30–60 mg of $Fe_2[(SCHR)_2\ NR](CO)_{4-x}(PMe_3)_x$ (x = 0, 2 and R = Me, H) in 20—30 mL of MeCN was treated with a stock solution of the acid in MeCN. Typically, the amines were treated with aliquots of 1 equiv of acid. Acid additions were continued, usually four to five aliquots, until the spectra of the protonated and unprotonated compounds could not be differentiated reliably. Using the WINFIRST program, spectra were converted to ASCII tables, which were imported into the Microcal-Origin, where the peaks were fit to Gaussian curves. Data were then imported into Microsoft Excel and adjusted visually for better individual peak fits. The pK_a values were then calculated using ratios of the peak areas for the highest frequency ν_{CO} peak (for additional details, see part 2 of the Supporting Information).

Computational Methods

DFT geometry optimizations have been carried out using the pure functional B-P86,[25] as implemented in TURBOMOLE,[26] in conjunction with a valence triple-ζ basis set with polarization on all atoms (TZVP).[27] Stationary points of the energy hypersurface have been located by means of energy gradient techniques, and full vibrational analysis has been carried out to further characterize each stationary point. Gibbs free energy (G) values have been obtained from the electronic SCF energy by considering three contributions to the total partition function (Q), namely $q_{translational}$, $q_{rotational}$, and $q_{vibrational}$, under the assumption that Q may be written as the product of such terms. In order to evaluate enthalpy and entropy contributions, the values for temperature and pressure have been set to 243.15 or 298.15 K and 1 bar, respectively, in order to reproduce experimental conditions. Rotations were treated classically.

X-ray Crystallography

Crystals were mounted using Paratone- N oil (Exxon) to a 0.3 mm cryoloop (Hampton Research). Data, collected at 193 K (for $Fe_2[(SCHMe)_2NH](CO)_6$ and $Fe_2[(SCHMe)_2NH](CO)_5(PPh_3)$) or 297 K (for $Fe_2[(SCH_2)_2NH](CO)_6$) on a Siemens CCD diffractometer, were filtered to remove statistical outliers. The integration software (SAINT) was used to test for crystal decay as a bilinear function of X-ray exposure time and sin θ. The data were solved using SHELXTL by direct methods; atomic positions were deduced from an E map or by an unweighted difference Fourier synthesis. H atom U values were assigned as $1.2U_{eq}$ for adjacent C atoms. Non-H atoms were refined anisotropically. Successful convergence of the full-matrix

least-squares refinement of F^2 was indicated by the maximum shift/error for the final cycle. For crystallographic data, see Table 3.

Acknowledgment

This research was supported by the NIH. We thank Nathan Eddingsaas for his assistance with the Gaussian fits.

References

1. Kubas, GJ. Metal Dihydrogen and σ-Bond Complexes. New York: Kluwer Academic/Plenum; 2001.
2. Frey M. ChemBioChem 2002;3:153–160. [PubMed: 11921392]
3. Vincent KA, Parkin A, Armstrong FA. Chem. Rev 2007;107:4366–4413. [PubMed: 17845060]Hu XL, Brunschwig BS, Peters JC. J. Am. Chem. Soc 2007;129:8988–8998. [PubMed: 17602556]Artero V, Fontecave M. Coord. Chem. Rev 2005;249:1518–1535.
4. Fontecilla-Camps JC, Volbeda A, Cavazza C, Nicolet Y. Chem. Rev 2007;107:4273–4303. [PubMed: 17850165]
5. Winter A, Zsolnai L, Huttner GZ. Naturforsch 1982;37b:1430–1436.Lyon EJ, Georgakaki IP, Reibenspies JH, Darensbourg MY. J. Am. Chem. Soc 2001;123:3268–3278. [PubMed: 11457062]
6. Justice AK, Rauchfuss TB, Wilson SR. Angew. Chem., Int 2007;46:6152–6154.Justice AK, Zampella G, De Gioia L, Rauchfuss TB. Chem. Commun 2007:2019–2021.Adam FI, Hogarth G, Richards I, Sanchez BE. Dalton Trans 2007:2495–2498. [PubMed: 17563784]Adam FI, Hogarth G, Richards I. J. Organomet. Chem 2007;692:3957–3968.Orain P-Y, Capon J-F, Kervarec N, Gloaguen F, Pétillon F, Pichon R, Schollhammer P, Talarmin J. Dalton Trans 2007:3754–3756. [PubMed: 17712440] Ezzaher S, Capon J-F, Gloaguen F, Pétillon FY, Schollhammer P, Talarmin J, Pichon R, Kervarec N. Inorg. Chem 2007;46:3426–3428. [PubMed: 17397148]Morvan D, Capon J-F, Gloaguen F, Le Goff A, Marchivie M, Michaud F, Schollhammer P, Talarmin J, Yaouanc J-J. Organometallics 2007;26:2042–2052.
7. Justice AK, Zampella G, De Gioia L, Rauchfuss TB, van der Vlugt JI, Wilson SR. Inorg. Chem 2007;46:1655–1664. [PubMed: 17279743]
8. Cao Z, Hall MB. J. Am. Chem. Soc 2001;123:3734–3742. [PubMed: 11457105]
9. Dong W, Wang M, Liu X, Jin K, Li G, Wang F, Sun L. Chem. Commun 2006:305–307.Zhao X, Chiang C-Y, Miller ML, Rampersad MV, Darensbourg MY. J. Am. Chem. Soc 2003;125:518–524. [PubMed: 12517165]Messelhäuser J, Gutensohn KU, Lorenz I-P, Hiller WJ. Organomet. Chem 1987;321:377–388.
10. Stanley JL, Rauchfuss TB, Wilson SR. Organometallics 2007;26:1907–1911.
11. Nielsen AT, Atkins RL, Moore DW, Scott R, Mallory D, LaBerge JM. J. Org. Chem 1973;38:3288–3295.
12. Lawrence JD, Li H, Rauchfuss TB, Bénard M, Rohmer M-M. Angew. Chem., Int. Ed 2001;40:1768–1771.
13. da Silva MAVR, Cabral JITA, Gomes P, Gomes JRB. J. Org. Chem 2006;71:3677–3685. [PubMed: 16674037]Baldock RW, Katritzky AR. J. Chem. Soc. B 1968:1470–1478.
14. Li H, Rauchfuss TB. J. Am. Chem. Soc 2002;124:726–727. [PubMed: 11817928]
15. Gao W, Liu J, Åkermark B, Sun L. J. Organomet. Chem 2007;692:1579–1583.Li P, Wang M, He C, Li G, Liu X, Chen C, Åkermark B, Sun L. Eur. J. Inorg. Chem 2005:2506–2513.
16. Schwartz L, Eilers G, Eriksson L, Gogoll A, Lomoth R, Ott S. Chem. Commun 2006:520–522.
17. Wang F, Wang M, Liu X, Jin K, Dong W, Sun L. Dalton Trans 2007:3812–3819. [PubMed: 17712448]
18. Wang F, Wang M, Liu X, Jin K, Dong W, Li G, Åkermark B, Sun L. Chem. Commun 2005:3221–3223.
19. Izutsu, K. Acid-Base Dissociation Constants in Dipolar Aprotic Solvents. Oxford, U.K.: Blackwell Scientific Publications; 1990.
20. Eilers G, Schwartz L, Stein M, Zampella G, de Gioia L, Ott S, Lomoth R. Chem. Eur. J 2007;13:7075–7084.
21. Pritchard JG, Vollmer RL. J. Org. Chem 1963;28:1545–1549.
22. Augustin-Nowacka D, Chmurzyñski L. Anal. Chim. Acta 1999;381:215–220.

23. Seyferth D, Henderson RS, Song L-C. J. Organomet. Chem 1980;192:C1–C5.
24. Bellachioma G, Cardaci G, Macchioni A, Reichenbach GJ. Organomet. Chem 1990;391:367–376.
25. Becke AD. Phys. Rev 1988;A38:3098–3100.Perdew JP. Phys. Rev 1986;B33:8822–8824.
26. Ahlrichs R, Baer M, Haeser M, Horn H, Koelmel C. Chem. Phys. Lett 1989;162:165–169.
27. Schaefer A, Huber C, Ahlrichs R. J. Chem. Phys 1994;100:5829–5835.

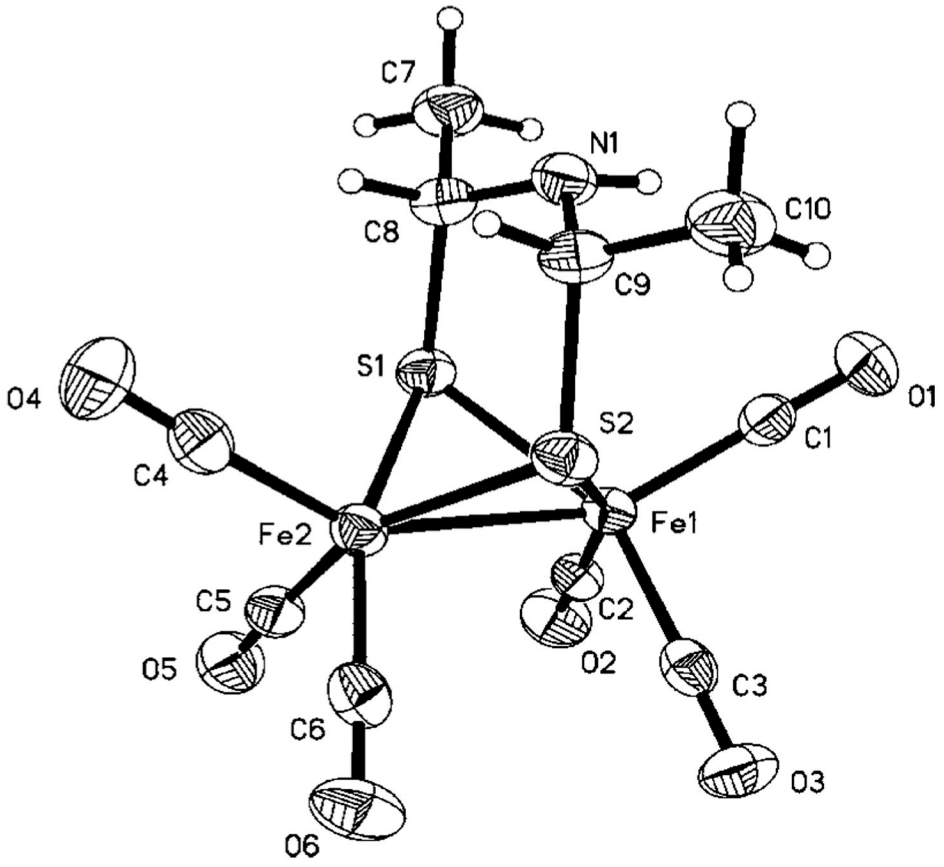

Figure 1.
Molecular structure of $Fe_2[(SCHMe)_2NH](CO)_6$ (**1**) with thermal ellipsoids drawn at the 50% probability level.

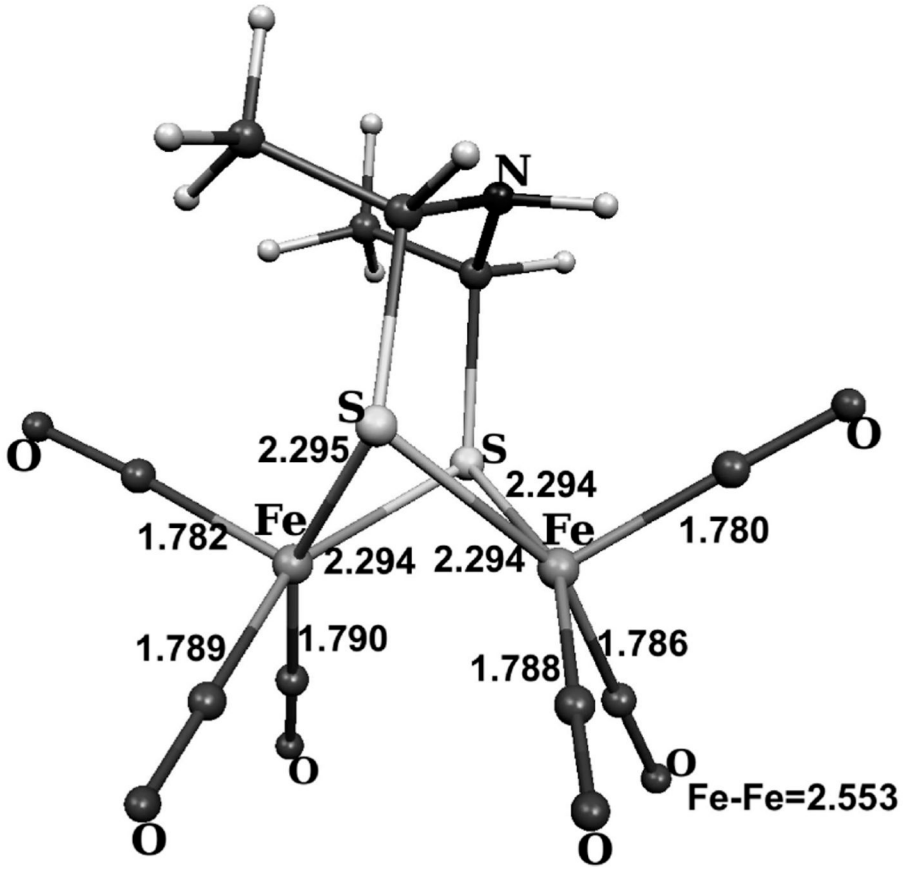

Figure 2.
DFT-optimized structure of the unstable conformer of *meso*-**1** with diaxial methyl groups.

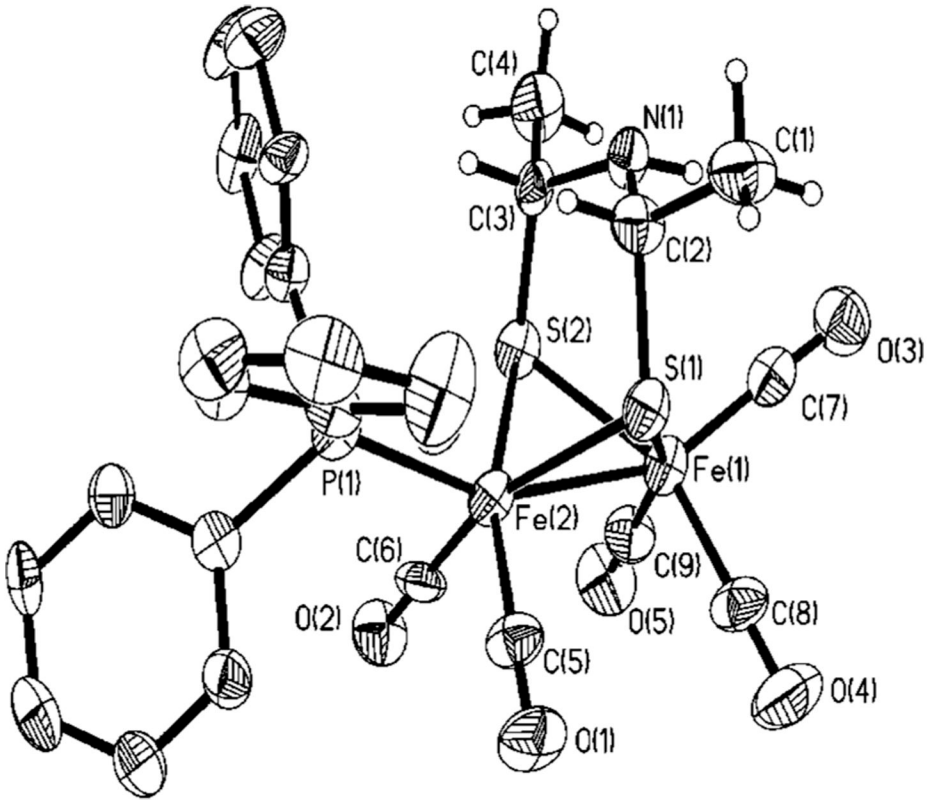

Figure 3.
Molecular structure of $Fe_2[(SCHMe)_2NH](CO)_5(PPh_3)$ with thermal ellipsoids drawn at the 50% probability level.

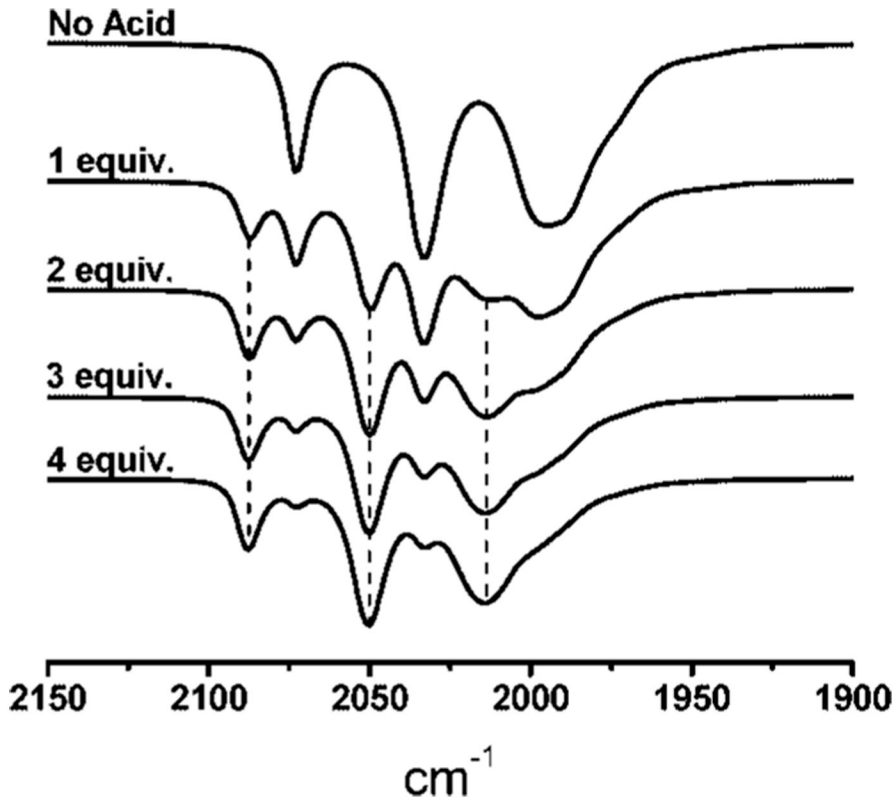

Figure 4.
IR spectra in the ν_{CO} region of $Fe_2[(SCHMe)_2NH](CO)_6$ displaying the effect of sequential additions of HOTs in a MeCN solution. The dotted lines indicate the band positions for the protonated species, $[Fe_2[(SCHMe)_2NH_2](CO)_6]^+$.

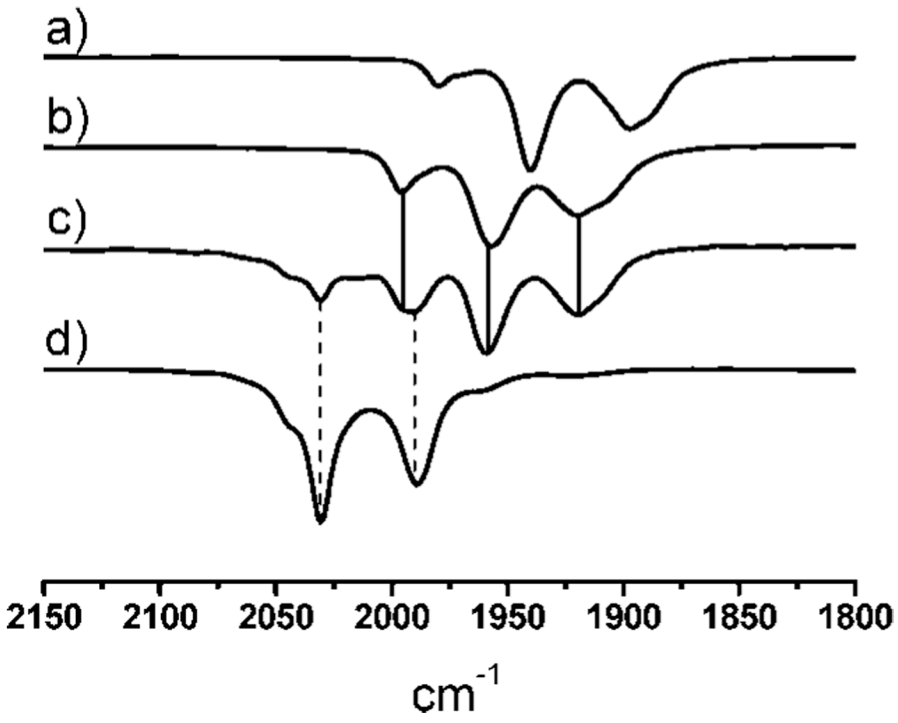

Figure 5.
IR spectra (MeCN solution) for the protonation of $Fe_2[(SCHMe)_2NH](CO)_4(PMe_3)_2$ with HOTs: (a) starting diiron complex; (b) $[Fe_2[(SCHMe)_2NH_2](CO)_4(PMe_3)_2]^+$; (c) same sample as in (b) after partial tautomerization to $[Fe_2[(SCHMe)_2NH](\mu\text{-}H)(CO)_4(PMe_3)_2]^+$; (d) $[Fe_2[(SCHMe)_2NH](\mu\text{-}H)(CO)_4(PMe_3)_2]^+$ (after addition of NH_4Cl).

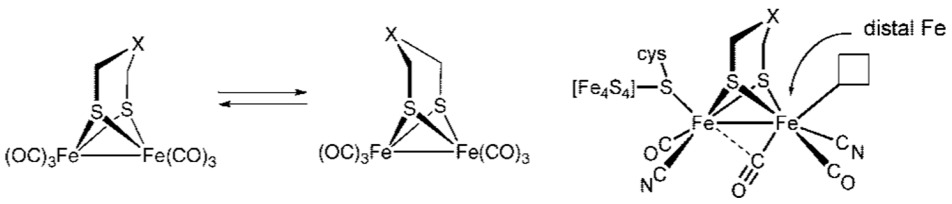

Scheme 1.

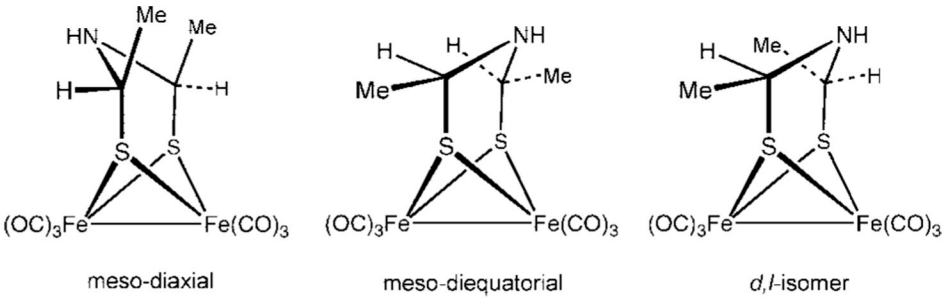

Scheme 2.

Table 1

Selected Bond Distances (Å) and Angles (deg) for $Fe_2[(SCHMe)_2NH](CO)_6$ (1), $Fe_2[(SCH_2)_2NH](CO)_6$, and $Fe_2[(SCHMe)_2NH](CO)_5(PPh_3)$

bond[a]	$Fe_2[(SCHMe)_2NH](CO)_6$	$Fe_2[(SCH_2)_2NH](CO)_6$	$Fe_2[(SCHMe)_2NH](CO)_5(PPh_3)$
Fe(1)—Fe(2)	2.5114(7)	2.5150(4)	2.512(2)
Fe(1)—S(1)	2.2686(10)	2.2584(4)	2.259(3)
Fe(1)—S(2)	2.2523(10)	2.2575(4)	2.271(3)
Fe(2)—S(1)	2.2485(10)	2.2584(4)	2.253(3)
Fe(2)—S(2)	2.2480(10)	2.2575(4)	2.260(3)
Fe(1)—CO_{ap}	1.797(4)	1.7948(14)	1.752(11)
Fe(2)—CO_{ap} (or PPh_3)	1.801(4)	1.7948(14)	2.226(3)
S(1)—CH	1.883(3)	1.8547(18)	1.846(10)
S(2)—CH	1.877(3)	1.861(2)	1.839(10)
C—N	1.412(4)	1.401(3)	1.439(11)
	1.428(4)	1.419(3)	1.426(11)
Fe—S—Fe	67.56(3)	67.671(15)	67.68(9)
	67.84(3)	67.703(15)	67.35(9)
S—Fe—S	56.60(3)	85.075(5)	84.01(10)
	56.16(3)		84.38(10)
HC—N—HC	119.3(3)	117.81(19)	116.1(8)

[a] CO_{ap} denotes an apical CO.

Table 2

pK_a Values for Diiron Azadithiolato Carbonyls Studied in This Work

Compound	pK_a(MeCN soln)
	7.98 ± 0.2
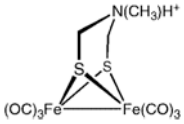	8.14 ± 0.37
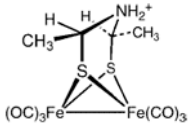	7.89 ± 0.16
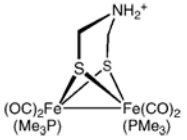	10.15 ± 0.14
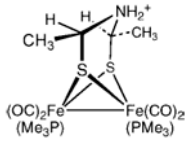	11.29 ± 0.64

Table 3

Crystallographic Data for $Fe_2[(SCHMe)_2NH](CO)_6$, $Fe_2[(SCH_2)_2NH](CO)_6$, and $Fe_2[(SCHMe)_2NH](CO)_5(PPh_3)$

	$Fe_2[(SCHMe)_2NH](CO)_6$	**$Fe_2[(SCH_2)_2NH](CO)_6$**	**$Fe_2[(SCHMe)_2NH](CO)_5(PPh_3)$**
chem formula	$C_{10}H_9Fe_2NO_6S_2$	$C_8H_5Fe_2NO_6S_2$	$C_{27}H_{24}Fe_2NPO_5S_2$
temp (K)	193(2)	297(2)	193(2)
cryst size (mm)	0.24 ± 0.14 ± 0.06	0.39 ± 0.22 ± 0.18	0.16 ± 0.06 ± 0.02
cryst syst	monoclinic	monoclinic	triclinic
space group	$P2_1/n$	$P2_1/m$	$P\bar{1}$
a (Å)	9.9640(13)	6.8441(7)	8.884(3)
b (Å)	12.0864(16)	13.6033(14)	10.484(4)
c (Å)	13.0405(17)	7.7636(8)	15.902(5)
α (deg)	90	90	93.118(5)
β (deg)	105.405(2)	108.980(2)	98.856(5)
γ(deg)	90	90	106.601(5)
V (Å^3)	1514.0(3)	683.51(12	1394.9(8)
Z	4	2	2
calcd density (Mg m^{-3})	1.821	1.880	1.546
μ(Mo Kα) (mm^{-1})	0.710 73	0.710 73	0.710 73
max/min transmissn	0.8838/0.6262	0.7095/0.5327	0.9759/0.7969
no. of measd/indep rflns	11 639/2783	9988/2870	13 556/3991
no. of data/restraints/params	2783/0/195	2870/2/101	3991/122/348
GOF on F^2	0.900	1.041	0.934
R_{int}	0.0528	0.0172	0.1461
R1 ($I > 2\sigma$) (all data)[a]	0.0337 (0.0617)	0.0239 (0.0322)	0.0715 (0.1721)
wR2 ($I > 2\sigma$) (all data)[b]	0.0646 (0.0701)	0.0600 (0.0641)	0.1365 (0.1717)
max peak/hole (e/Å^3)	0.578/−0.424	0.320/−0.254	0.839/−0.429

[a] $R1 = \Sigma||F_O| - |F_C||/\Sigma|F_O|$.

[b] $wR2 = \{\Sigma w(|F_O| - |F_C|)^2]/\Sigma\,[wF_O^2]\}^{1/2}$, where $w = 1/\sigma^2\,(F_O)$.